Photoelectron Spectroscopy of the NCN^- and $HNCN^-$ Ions

Eileen P. Clifford,[†] Paul G. Wenthold,[†,‡] W. Carl Lineberger,[†,‡] George A. Petersson,[§] and G. Barney Ellison*[,†]

Department of Chemistry & Biochemistry, University of Colorado, Boulder, Colorado 80309-0215, JILA, University of Colorado, Boulder, Colorado 80309-0440, and Hall Atwater Laboratories of Chemistry, Wesleyan University, Middletown, Connecticut 06459

Received: December 13, 1996; In Final Form: March 10, 1997[⊗]

We have used negative ion photoelectron spectroscopy to measure the electron affinities of the cyanonitrene and the cyanoamino radical: EA($\tilde{X}\ ^3\Sigma_g^-$ NCN) = 2.484 ± 0.006 eV, EA($\tilde{X}\ ^2A''$ HNCN) = 2.622 ± 0.005 eV, and EA($\tilde{X}\ ^2A''$ DNCN) = 2.622 ± 0.005 eV. Our experimental findings are accurately reproduced by complete basis set (CBS) *ab initio* electronic structure calculations: EA($\tilde{X}\ ^3\Sigma_g^-$ NCN) = 2.51 ± 0.03 eV and EA($\tilde{X}\ ^2A''$ HNCN) = 2.60 ± 0.03 eV. Our qualitative picture of these species is N═C═N $\tilde{X}\ ^3\Sigma_g^-$, $[N{=}C{=}N]^-$ $\tilde{X}\ ^2\Pi_u$, HNC≡N $\tilde{X}\ ^2A''$, and $[HNC{\equiv}N]^-$ $\tilde{X}\ ^1A'$. We make use of the electron affinities of NCN and HNCN, together with the gas phase acidity of cyanamide, $\Delta_{acid}H_{298}$(H−NHCN) = 350 ± 3 kcal mol^{-1}, to find the bond enthalpies of H_2NCN. We find DH_{298}(H−NHCN) = 96.9 ± 3.0 kcal mol^{-1} and Δ_fH_{298}(HNCN) = 77 ± 4 kcal mol^{-1}, which closely agree with the calculated values: DH_{298}(H−NHCN) = 95.5 ± 0.7 kcal mol^{-1} and Δ_fH_{298}(H−NCN) = 76.7 ± 0.7 kcal mol^{-1}. We therefore use the CBS *ab initio* electronic structure calculations to estimate $\Delta_{acid}H_{298}$(H−NCN) ≅ 339 kcal mol^{-1}. Use of the experimental electron affinity, EA(NCN), leads to the NH bond enthalpy of the cyanoamino radical, DH_{298}(H−NCN) = 83 ± 2 kcal mol^{-1} and Δ_fH_{298}(NCN) = 108 ± 4 kcal mol^{-1}.

I. Introduction

The NCN and HNCN radicals are interesting derivatives of the amidogen (NH) and amino (NH_2) radicals because the cyano group is likely to stabilize the unpaired electrons. Both of these species are also possible reactive intermediates in the chemistry of "active nitrogen". Cyanonitrene, NCN, was first implicated as an important intermediate in combustion chemistry in 1960, when a complicated emission at 329 nm was observed from hydrocarbon flames.[1]

An important experimental means to study the neutral radicals (M) is to photodetach mass-selected beams of the corresponding negative ions (M^-). We have used negative ion photoelectron spectroscopy to study both the NCN^- and $HNCN^-$ ions.

$$NCN^- + \hbar\omega_{351nm} \rightarrow NCN + e^- \qquad (1a)$$

$$HNCN^- + \hbar\omega_{351nm} \rightarrow HNCN + e^- \qquad (1b)$$

Our photoelectron spectra provide the molecular electron affinities EA(NCN) and EA(HNCN). Use of the EAs along with the gas phase acidities of the corresponding cyanamides enables us to determine the thermochemistry of the NCN and HNCN radicals. Our findings are accurately predicted by *ab initio* electronic structure calculations; our CBS (complete basis set) calculations[2−4] completely describe the geometries and energetics of the [NCN^-, $HNCN^-$] ions and [NCN, HNCN] radicals.

We can anticipate the structures and states of both species by use of the following diagrams.[5] Cyanonitrene is a diradical and will have three low-lying states, $\tilde{X}\ ^3\Sigma_g^-$, $\tilde{a}\ ^1\Delta_g$, and $\tilde{b}\ ^1\Sigma_g^+$, as well as a pair of Π states, $\tilde{A}\ ^3\Pi_u$ and $\tilde{c}\ ^1\Pi_u$. The triplet state is expected to be the ground state, $\tilde{X}\ ^3\Sigma_g^-$, and one can write this as a resonating formula:

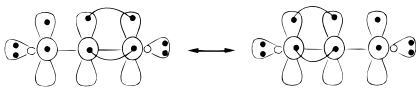

N=C=N $\tilde{X}\ ^3\Sigma_g^-$ (2)

The lowest singlet state will be $\tilde{a}\ ^1\Delta_g$; the $^1\Delta_g^-$ component might be represented as

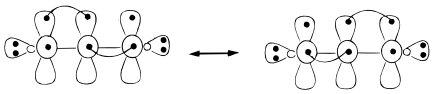

N=C=N $\tilde{a}\ ^1\Delta_g$ (3)

The negative ion, NCN^-, is isoelectronic with NCO and is anticipated to be a $^2\Pi_u$ state:

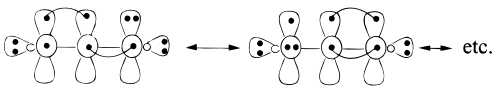

$N{=}C{=}N^-$ $\tilde{X}\ ^2\Pi_u$ (4)

Formulae 4 and 2 suggest that there will be little geometry change upon detachment of the NCN^- ion. The electron affinity of NH is very well known[6,7] from spectroscopic studies of the NH^- ion, X $^2\Pi$, and it is found that EA(NH) is 0.370 ± 0.004 eV. We expect the CN group to stabilize the anion by about 1 eV while resonance effects will stabilize the ion even further. Consequently we anticipate a nearly vertical photodetachment spectrum for NCN as in NH, with an EA(NCN) of roughly 2 eV.

The amino radical, NH_2, has a $\tilde{X}\ ^2B_1$ ground state and a low-lying[8] excited state, $\tilde{A}\ ^2A_1$; T_0($\tilde{A}$ NH_2) = 1.271 eV. We

[†] Department of Chemistry & Biochemistry, University of Colorado.
[‡] JILA, University of Colorado.
[§] Wesleyan University.
[⊗] Abstract published in *Advance ACS Abstracts,* April 15, 1997.

S1089-5639(96)04067-4 CCC: $14.00

anticipate that the HNCN radical will have a $\tilde{X}\ ^2A''$ ground state and an $\tilde{A}\ ^2A'$ excited state.

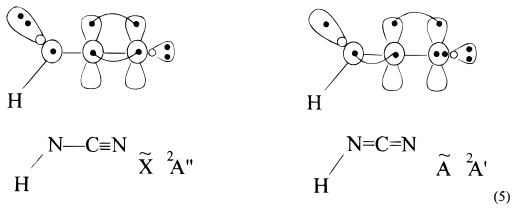

(5)

One would write the $HNCN^-$ ion as a closed shell species, $\tilde{X}\ ^1A'$:

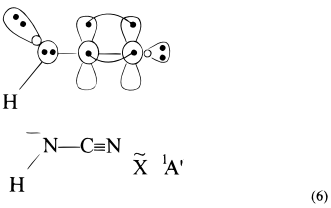

(6)

The photoelectron spectrum of the amide ion has been studied[9] and it was found that $EA(NH_2) = 0.771 \pm 0.006$ eV. Again we anticipate the cyano group to stabilize the negative ion and estimate EA(HNCN) $\cong$ 2 eV. A nearly vertical photodetachment spectrum is expected as well since detachment of the $\tilde{X}\ ^1A'$ $HNCN^-$ ion in (6) involves ejection of a nonbonding electron.

The NCN and HNCN radicals have been studied previously. The gas phase optical spectrum of the NCN radical has been obtained following the photolysis of diazomethane.[10] A rotational analysis of the bands indicated a triplet/triplet absorption at 30 383.74 cm^{-1} which was assigned as NCN ($\tilde{A}\ ^3\Pi_u \leftarrow \tilde{X}\ ^3\Sigma_g^-$). From the rotational constant, $B_0'' = 0.3968$ cm^{-1}, the C═N bond length was reported to be $r_o(\tilde{X}\ ^3\Sigma_g^-$ NCN) = 1.232 Å. Very recently[11] laser-induced fluorescence (LIF) spectra have yielded a set of refined rotational constants and show the excited Π state to be inverted, $\tilde{A}\ ^3\Pi_{u\ 3/2}$. From the optical spectrum, the NCN bending frequency was estimated to be $\nu_2'' = 370 \pm 50$ cm^{-1}. Subsequently NCN $\tilde{X}\ ^3\Sigma_g^-$ was detected by EPR spectroscopy[12] in a matrix at 4 K. Singlet states of NCN have been observed[13,14] by flash photolysis as well; T_0 ($^1\Pi_u \leftarrow$ $\tilde{a}\ ^1\Delta_g$ NCN) = 30 046 cm^{-1}. Some hints of UV transitions originating from NCN $\tilde{b}\ ^1\Sigma_g^+$ have also been reported.[15] Dynamical studies of the quenching of NCN ($\tilde{A}\ ^3\Pi_u \rightarrow \tilde{X}\ ^3\Sigma_g^-$) have been reported[16] and the lifetime of NCN $\tilde{A}\ ^3\Pi_u$ was measured to be 183 $\pm$ 6 ns. To the best of our knowledge, no singlet/triplet splittings have been measured.

The infrared absorption spectrum of NCN was measured[17] in a N_2 matrix at 14−20 K following irradiation of cyanogen azide. Analysis of the IR spectrum yielded values[18] for the bending frequency, $\nu_2 = 423 \pm 3$ cm^{-1}, and the asymmetric stretch, $\nu_3 = 1475 \pm 3$ cm^{-1}; the IR inactive symmetric stretch was estimated to be $\nu_1 \cong 808$ cm^{-1}. These matrix studies suggest that irradiation of NCN at wavelengths below 2800 Å leads to dissociation to produce molecular nitrogen: NCN ($\tilde{X}\ ^3\Sigma_g^-$) + ($\hbar\omega \cong 4.4$ eV) → C (^3P) + N_2 ($^1\Sigma_g^+$). In subsequent studies,[19] matrix spectroscopy revealed a weak band at 2672 cm^{-1} which was interpreted as a combination ($\nu_1 + \nu_3$); this provided a refined value for ν_1(NCN) = 1197 cm^{-1}. Very recent gas phase FTIR absorption studies in a White cell following pyrolysis of NCN_3 with a CO_2 laser have provided values[20] for the two IR allowed bands for NCN $\tilde{X}\ ^3\Sigma_g^-$: $\nu_2 \cong$ 395 cm^{-1} and $\nu_3 = 1466.5$ cm^{-1}. Besides these experimental studies, the NCN molecule has been studied by *ab initio* electronic structure calculations.[21,22] A quadratic CI calculation [UHF-QCISD/6-31G*] has yielded[23] harmonic frequencies for NCN $\tilde{X}\ ^3\Sigma_g^-$. All of these results are summarized in Table 1.

TABLE 1: Molecular Constants for NCN

state	B_0/cm^{-1}	r/Å	T_0/cm^{-1}	ref
$\tilde{X}\ ^3\Sigma_g^-$	0.396 8	1.232	−	10
$\tilde{X}\ ^3\Sigma_g^-$	0.397 252 2 ± 0.000 008 7	1.230 944 ± 0.000 014	−	11
$\tilde{A}\ ^3\Pi_u$	0.396 2	1.233	30 383.74	10
$\tilde{A}\ ^3\Pi_u$	−	−	30 384	17
$\tilde{A}\ ^3\Pi_u$	−	−	30 395 ± 9	16
$\tilde{A}\ ^3\Pi_{u\ 3/2}$	0.396 645 2 ± 0.000 008 7	1.231 866 ± 0.000 014	30 383.967 06 ± 0.000 49	11

state	sym st, ν_1/cm^{-1}	bend, ν_2/cm^{-1}	asym st, ν_3/cm^{-1}	ref
$\tilde{X}\ ^3\Sigma_g^-$ (matrix)	−	423 ± 3	1475 ± 3	18
$\tilde{X}\ ^3\Sigma_g^-$ (matrix)	1197	−	−	19
$\tilde{X}\ ^3\Sigma_g^-$	−	≅395	1466.5	20
$\tilde{X}\ ^3\Sigma_g^-$	−	−	1466.507 530 ± 0.000 091	44
$\tilde{A}\ ^3\Pi_u$	1154	−	−	14
$\tilde{c}\ ^1\Pi_u$	1160	−	−	14
$^3\Sigma_u^-$	1100	−	−	14

Ab Initio Electronic Structure Calculations for NCN $\tilde{X}\ ^3\Sigma_g^-$

calculation	energy/au	$\langle S^2\rangle$	r_{CN}/Å	B_0/cm^{-1}	ref
UHF/DZP	−146.694 95	−	1.196	−	21
RHF/(9s,5p,1d/4s,2p,1d)	−146.679 87	−	1.197	−	22
UHF-QCISD/6-31G*	−	−	1.245	−	23
CCSD(T)/TZ2P	−147.250 48	2.052	1.233	0.396	45

Harmonic Vibrational Frequencies (Unscaled) and IR Intensities: ω/cm^{-1} [A/km mol^{-1}]

species	ω_1/NCN sym. st	ω_2/NCN bend	ω_3/NCN asym st	ref
NCN	1247	437	1411	23
NCN	1234 [0]	357 [29]	1328 [294]	45

The cyanoamino radical has also been studied previously. The absorption spectrum of the HNCN radical at 344.0 nm was detected in 1963 following flash photolysis of diazomethane.[24] Rotational analysis revealed the transition to be HNCN $\tilde{A}\ ^2A'$ ← HNCN $\tilde{X}\ ^2A''$. Both the upper and lower electronic states were found to be planar molecules. More recently the LIF spectrum of jet-cooled HNCN was reported[25] following 193 nm irradiation of a mixture of NH_3, NCCN, and N_2. The HNCN radical was likely formed by the reaction CN + NH_2 → HNCN + H. The LIF spectrum was analyzed to yield $T_0(\tilde{A}\ ^2A'$ HNCN) = 28 993.766 ± 0.018 cm^{-1} and the lifetime of HNCN $\tilde{A}\ ^2A'$ was found to be 20 ± 5 ns. Table 2 collects the molecular constants of the HNCN radical. A careful *ab initio* electronic structure calculation has been reported for the HNCN radical.[26] This MP2 calculation in a 6-311G(2d,2p) basis gave the rotational constants and harmonic vibrations for HNCN and the results are collected in Table 2.

II. Experimental Procedures

Our photoelectron spectra were taken on a spectrometer that has been described elsewhere.[27,28] We have used oxide ion chemistry[29] to generate the NCN^- from cyanamide; NH_2CN was acquired from Aldrich Chemical and used without further purification. The chemistry used to produce our target ions is

$$O^- + NH_2CN \rightarrow OH_2 + NCN^- \quad (m/z\ 40) \qquad (7a)$$

$$OH^- + NH_2CN \rightarrow OH_2 + HNCN^- \quad (m/z\ 41) \qquad (7b)$$

TABLE 2: Molecular Constants for HNCN

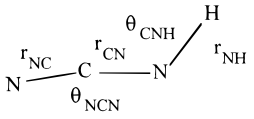

$\tilde{X}\ ^2A''$

A_0/GHz	B_0/GHz	C_0/GHz	ref
634.900 ± 3.100	11.087 813 4 ± 0.000 009 8	10.881 713 5 ± 0.000 010 1	46
638.5 ± 0.7	11.1 ± 0.7	10.9 ± 0.7	25
636.2	11.1	10.9	24
r_{NCN} = 2.470 ± 0.002 Å; r_{NH} = 1.034 ± 0.020 Å; θ_{CNH} = 116.5° ± 2.7°			24
ν_3/N−C−N sym st/a′ ≅ 1140 cm^{-1}			25
ν_6/N−C−N out-of-plane bend/a″ ≅ 440 cm^{-1}			25

$\tilde{A}\ ^2A'$

ν_0/cm^{-1}	A_0/GHz	B_0/GHz	C_0/GHz	ref
28 993.766 ± 0.018	668.5 ± 0.3	11.3 ± 0.7	11.1 ± 0.7	25
28 994.13	672.7	11.3	11.1	24
r_{NCN} = 2.443 ± 0.002 Å; r_{NH} = 1.035 ± 0.022 Å; θ_{CNH} = 120.6° ± 2.5°				24

Ab Initio Electronic Structure Calculations for $\tilde{X}\ ^2A''$

		harmonic vibrational frequencies (unscaled) and IR intensities	
MP2/6-311G(2d,2p)[a]		ω/cm^{-1}	A/km mol^{-1}
r_{NC}/Å = 1.166	ω_1(a′)/N−H st	3552	43
r_{CN}/Å = 1.291	ω_2(a′)/NCN a st	1937	73
r_{NH}/Å = 1.017	ω_3(a′)/NCN s st	1179	118
θ_{NCN} = 175.0°	ω_4(a′)/HNC bend	981	12
θ_{CNH} = 110.8°	ω_5(a′)/NCN bend	526	22
	ω_6(a″)/NCN bend	535	13
A_e/GHz = 628.0			
B_e/GHz = 11.2			
C_e/GHz = 11.1			
energy/au = −147.779 82			

[a] MP2 calculations from ref 26.

The two ions at *m*/*z* 40 and 41 were separated by a Wien velocity filter and were photodetached by a CW Ar III ion laser that provides 50−100 W of 351.1 nm light in the circulating build-up cavity. The photodetached electrons are focused and pass through a hemispherical energy analyzer, with an instrumental resolution (FWHM) of 6−10 meV. In order to reduce rotational broadening in the photodetachment spectra, we bathe part of the flow tube with liquid N_2. We estimate (*vide infra*) that the rotational temperature of our ions is roughly 200 K. The deuterated precursor, D_2NCN, was prepared by washing the H_2NCN with methanol-d_1 (CH_3OD) and evaporating the solvent; the extent of D_2NCN formation was verified by electron impact mass spectrometry.

Our photoelectron spectra are calibrated[30] with respect to O^- and transformed to the center of mass (CM) frame by a standard[31] expression where E is the CM kinetic energy (eV) of an electron detached from an ion of mass M (amu) which is passed by the energy analyzer when the slit voltage is V. The beam energy is W, m_e is the mass of an electron, and γ is the dimensionless scale compression factor (typically 1.000 ± 0.006):

$$E = E_{cal} + \gamma(V - V_{cal}) + m_e W\left(\frac{1}{M_{cal}} - \frac{1}{M}\right)$$

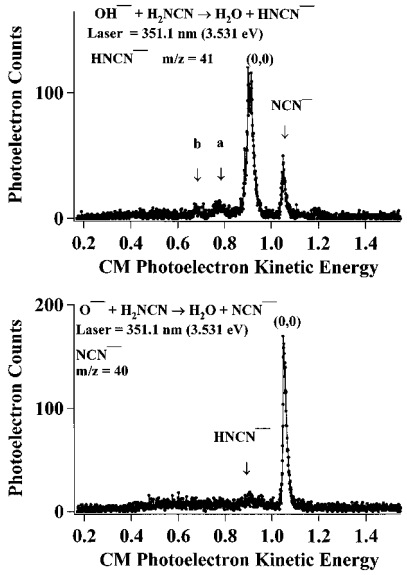

Figure 1. (a) Negative ion photoelectron spectrum of the $HNCN^-$ ion; the (0,0) feature occurs at a electron kinetic energy of 0.909 ± 0.002 eV. (b) Negative ion photoelectron spectrum of the NCN^- ion: the (0,0) feature occurs at a electron kinetic energy of 1.052 ± 0.003 eV.

III. Results

Figure 1 presents the photoelectron spectrum of the $HNCN^-$ ion on the top panel and the NCN^- ion on the bottom. Because of limited mass-resolution, each spectrum is slightly contaminated with the other ion. The $HNCN^-$ ion (*m*/*z* 41) is prepared by reaction of cyanamide with hydroxide ion while the NCN^- species (*m*/*z* 40) results from the interaction of oxide anion with cyanamide. As expected from eqs 2 and 4 and 5 and 6, both photoelectron spectra are essentially vertical transitions. The intense feature in the $HNCN^-$ spectrum is the (0,0) band for HNCN $\tilde{X}\ ^2A'' \leftarrow HNCN^-\ \tilde{X}\ ^1A'$, and it occurs at center-of-mass kinetic energy = 0.908 ± 0.002 eV. This corresponds to a value for the uncorrected or "raw" EA(HNCN) = 2.623 ± 0.002 eV. The strong band in the NCN^- spectrum is the (0,0) transition for NCN $\tilde{X}\ ^3\Sigma_g^- \leftarrow NCN^-\ \tilde{X}\ ^2\Pi_g$ occurring at center-of-mass kinetic energy = 1.052 ± 0.003 eV and corresponding to a "raw" EA(NCN) = 2.479 ± 0.003 eV.

The yields of photodetached electrons are angular dependent. The distribution of scattered photoelectrons, $I(\theta)$, is approximated[32,33] by the following expression.

$$I(\theta) = \frac{\bar{\sigma}}{4\pi}\left(1 + \frac{\beta(3\cos^2\theta - 1)}{2}\right) \qquad (8)$$

In this expression, θ is the angle between $\mathbf{E}_{laser}$ and the electron collection direction, $\bar{\sigma}$ is the average photodetachment cross section, and β is the anisotropy factor. The anisotropy factor β can vary from −1 to 2 ($-1 \le \beta \le 2$). The photoelectron spectra shown in Figure 1 were collected under conditions where θ was set to the "magic angle" of 54.7° so that $I(\theta) = \bar{\sigma}/4\pi$ and is independent of β. If spectra are collected at $\theta = 0°$ ($\mathbf{E}_{laser}$ and collection direction ||) and $\theta = 90°$ ($\mathbf{E}_{laser}$ and collection direction ⊥), one can extract a value for the anisotropy factor.

$$\beta \cong \frac{I_{0°} - I_{90°}}{\frac{1}{2}I_{0°} + I_{90°}} \qquad (9)$$

The value of β provides an important clue as to the nature of the photodetached electron. In atoms, detachment of an

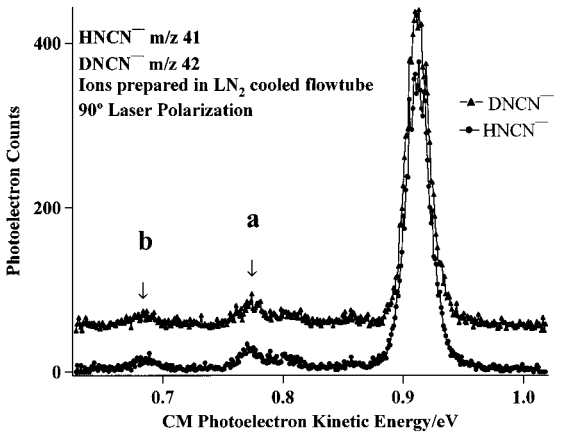

Figure 2. An overlay of the negative ion photoelectron spectra of $HNCN^-$ (●) and $DNCN^-$ (s). Feature a is split from the origin by 1049 ± 177 cm^{-1} and is assigned 3_0^1 while peak b is split from the (0,0) band by 1813 ± 128 cm^{-1} and is assigned as 2_0^1.

s-electron leads to an outgoing p-wave ($l = 1$) and $\beta = 2$, independent of electon kinetic energy. Detachment of a p-electron results in a mixture of interfering s- and d-waves and leads to an energy dependent value for β. At photodetachment threshold, s-wave ($l = 0$) detachment dominates, giving $\beta = 0$ and yielding an isotropic photoelectron angular distribution. At photoelectron kinetic energies roughly 1 eV above threshold, d-wave detachment becomes important and $\beta \rightarrow -1$. Electron detachment from molecular ions is more complicated than the atomic case, but β is generally found to be positive for detachment from σ (s-like) electrons and negative for detachment from π (p-like) orbitals. Use of (9) leads to the following anisotropy factors; β(NCN) = −0.59 ± 0.15 and β(HNCN) = −0.53 ± 0.15. Both β values are suggestive of ejection of a π-like electron from both the NCN^- and $HNCN^-$ anions and are in qualitative agreement with our pictures of these negative ions in eqs 4 and 6.

There are two small features in the $HNCN^-$ spectrum and we ascribe them to vibrational excitation in the HNCN radical. To identify these modes, we need to compare the spectrum of the d_0 and the d_1 ions. Figure 2 is an overlay of the photoelectron spectra of $HNCN^-$ and $DNCN^-$. The two small features at a and b correspond to vibrational excitations in the cyanoamino radical. Since these two spectra are identical, the HNCN/DNCN vibrations a and b do not involve motion of either the H or D atoms. The splitting of a from the (0,0) band is 1049 ± 177 cm^{-1} while that of b is 1813 ± 128 cm^{-1}. On the basis of the earlier[25] LIF assignment ($\nu_3 \cong 1140$ cm^{-1}), we assign our feature a as ν_3, the symmetric HN−C−N stretch. Our B3LYP *ab initio* electronic structure calculations[34] (*vide infra*) listed in Table 4 find a harmonic frequency of $\omega_3 = 1202$ cm^{-1}. The only reasonable assignment for b is ν_2, the asymmetric HN−C−N stretch for which the B3LYP calculation predicts $\omega_2 = 1902$ cm^{-1}. Based on our view of HNCN $\tilde{X}$ $^2A''$ and $HNCN^-$ $\tilde{X}$ $^1A'$ in eqs 5 and 6, activation of modes ν_2 and ν_3 following detachment is expected.

In order to interpret our photoelectron spectra, we need a consistent set of molecular geometries and vibrational frequencies of the NCN and HNCN radicals as well as for the NCN^- and $HNCN^-$ ions. In addition to the earlier *ab initio* electronic structure calculations, we report the results of our own density functional calculations. These are B3LYP calculations in a 6-311++G(2df,p) basis.[34] The B3LYP/6-311++G(2df,p) calculations give us a balanced set of results with which to compare the negative ion and the neutral, and these findings are collected in Table 4.

TABLE 3: Photoelectron Bands

feature	com kinetic energy/eV	assignment
		HNCN[b]
(0,0)	0.908 ± 0.002	EA($\tilde{X}$ $^2A''$ HNCN)
a	0.778 ± 0.020	ν_3($\tilde{X}$ $^2A''$ HNCN) = 1049 ± 162 cm^{-1}
b	0.675 ± 0.013	ν_2($\tilde{X}$ $^2A''$ HNCN) = 1879 ± 106 cm^{-1}
		DNCN
(0,0)	0.908 ± 0.002	EA($\tilde{X}$ $^2A''$ DNCN)
a	0.779 ± 0.020	ν_3($\tilde{X}$ $^2A''$ DNCN) = 1049 ± 162 cm^{-1}
b	0.684 ± 0.013	ν_2($\tilde{X}$ $^2A''$ DNCN) = 1879 ± 106 cm^{-1}
		NCN[a]
(0,0)	1.052 ± 0.003	EA($\tilde{X}$ $^3\Sigma_g^-$ NCN)

[a] The features for NCN are reproducible within ±0.003 eV and this molecule requires a rotational correction[47] (Δ_{rot} = 0.0004 eV), a spin-orbit correction (0.005 eV), and accommodation for the uncertainty in the energy linearity of the analyzer (0.005 eV). Consequently we apply the correction: raw EA(NCN) = EA(NCN) − $\langle E'' \rangle$ + $\langle E' \rangle$ − $\Delta_{spin-orbit}$ or EA(NCN) = raw EA(NCN) − Δ_{rot} + $\Delta_{spin-orbit}$. Applying these corrections, we find EA($\tilde{X}$ $^3\Sigma_g^-$ NCN) = 2.484 ± 0.006 eV or 57.3 ± 0.1 kcal mol^{-1}. [b] The transitions of HNCN are reproducible within ±0.002 eV and this molecule requires a rotational correction (Δ_{rot} = 0.001 eV) and no spin-orbit correction. Consequently we apply the correction: EA(HNCN) = raw EA(HNCN) − Δ_{rot}. Applying these corrections, we find EA($\tilde{X}$ $^2A''$ HNCN) = 2.622 ± 0.005 eV (60.5 ± 0.1 kcal mol^{-1}) and EA($\tilde{X}$ $^2A''$ DNCN) = 2.622 ± 0.005 eV (60.5 ± 0.1 kcal mol^{-1}).

These B3LYP/6-311++G(2df,p) calculations largely reproduce the experimental findings in Table 1. The ground state NCN $\tilde{X}$ $^3\Sigma_g^-$ is calculated to be very nearly a triplet with $\langle S^2 \rangle$ = 2.052 instead of the required value of 2 and the CN distance is found to be slightly smaller (1.224 Å) than the experimental value of 1.232 Å. The B3LYP harmonic frequencies for NCN $\tilde{X}$ $^3\Sigma_g^-$ are also qualitatively correct. We find unscaled frequencies of $\omega_1 = 1274$ cm^{-1}, $\omega_2 = 453$ cm^{-1}, and $\omega_3 = 1557$ cm^{-1}, which can be compared with the experimental values in Table 1 of $\nu_1 = 1197$ cm^{-1}, $\nu_2 \cong 395$ cm^{-1}, and $\nu_3 = 1466.5$ cm^{-1} (notice that the value for ν_1 is measured in a matrix). As predicted by eq 4, the properties of the NCN^- $\tilde{X}$ $^2\Pi_u$ ion are computed in Table 4 to be very close to those of the NCN $\tilde{X}$ $^3\Sigma_g^-$ neutral species.

Likewise the properties of the HNCN $\tilde{X}$ $^2A''$ radical are found to be qualitatively correct. In Table 2 the UV spectroscopists report a larger CNH angle of θ = 116.5° ± 2.7° than we compute (113.6°) while the sum of the heavy atom distances is found to be 2.470 ± 0.002 Å, which is to be compared to the value found by the B3LYP calculation of 2.458 Å [= 1.188 Å + 1.270 Å]. The GVB picture of HNCN $\tilde{X}$ $^2A''$ in (5) is essentially HNC≡N with a short HNC≡N bond and a longer HN−CN length.[35] Our DFT *ab initio* calculation leads to an N−H bond length of 1.022 Å, which is to be compared with the experimental finding of 1.034 ± 0.020 Å. The only vibrational frequencies found for HNCN $\tilde{X}$ $^2A''$ are $\nu_3 \cong 1140$ cm^{-1} and $\nu_6 \cong 440$ cm^{-1}; these values are plausibly close to the B3LYP harmonic frequencies of $\omega_3 = 1202$ cm^{-1} and $\omega_6 = 474$ cm^{-1}. Our qualitative description for the $HNCN^-$ ion in (6) is compatible with the *ab initio* results in Table 4.

We can model the rotational contours of our photoelectron spectra for both NCN^- and $HNCN^-$. The peak shapes that we observe in Figure 1 are due to a convolution of the rotational envelope with our instrumental resolution. Since the center of the peak does not correspond with the (0,0) rotational transition, we estimate the true (0,0) transition from a simulation of the rotational contour which requires a rotational temperature and

TABLE 4: *Ab Initio* Electronic Structure Calculations of Equilibrium Geometries and Vibrational Frequencies

B3LYP/6-311++G(2df,p) DFT Calculations

species	energy/au	$\langle S^2 \rangle$	r_{CN}/Å	B_e/cm^{-1}
NCN $\tilde{X}\ ^3\Sigma_g^-$	−147.541 18	2.061	1.224	0.402
NCN^- $\tilde{X}\ ^2\Pi_u$	−147.634 57	0.771	1.230	0.398

Harmonic Vibrational Frequencies (Unscaled) and IR Intensities: ω/cm^{-1} [A/km mol^{-1}]

species	ω_1/NCN sym st	ω_2/NCN bend	ω_3/NCN asym st
NCN	1274 [0]	453 [19]	1557 [202]
NCN^-	1265 [0]	530 [22]	1675 [118]

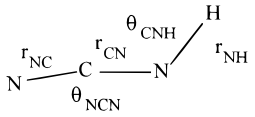

	B3LYP/6-311++G(2df,p)			B3LYP/6-311++G(2df,p)	
	HNCN $\tilde{X}\ ^2A''$	$HNCN^-$ $\tilde{X}\ ^1A'$		HNCN $\tilde{X}\ ^2A''$	$HNCN^-$ $\tilde{X}\ ^1A'$
r_{NC}/Å	1.188	1.183	A_e/GHz	652.4	628.4
r_{CN}/Å	1.270	1.298	B_e/GHz	11.1	11.0
r_{NH}/Å	1.022	1.017	C_e/GHz	11.0	10.8
θ_{NCN}	174.2°	174.9°	energy/au	−148.183 63	−148.278 28
θ_{CNH}	113.6°	111.0°	$\langle S^2 \rangle$	0.772	0

Harmonic Vibrational Frequencies (Unscaled) and IR Intensities: ω/cm^{-1} [A/km mol^{-1}]

	ω_1(a′) N−H st	ω_2(a′) NCN a st	ω_3(a′) NCN s st	ω_4(a′) HNC bend	ω_5(a′) NCN bend	ω_6(a″) NCN bend
HNCN	3466 [39]	1902 [07]	1202 [02]	1059 [98]	500 [20]	474 [08]
DNCN	2536 [20]	1894 [04]	1181 [02]	855 [42]	460 [22]	469 [16]
$HNCN^-$	3469 [14]	2149 [736]	1172 [16]	1112 [154]	541 [23]	612 [01]

rotational constants of the anion and the neutral species.[9] We adopt (a) the known rotational constants for HNCN $\tilde{X}\ ^2A''$ in Table 2 [$A_0' = 21.2 \pm 0.1$ cm^{-1}, $B_0' = 0.369\,849\,6 \pm 0.000\,000\,3$ cm^{-1}, $C_0' = 0.362\,974\,8 \pm 0.000\,000\,3$ cm^{-1}], (b) $T_{rot} = 200$ K, and (c) an instrumental linewidth (FWHM) of 10 meV. We can account for the linewidth of the $HNCN^-$ spectrum if we adopt the B3LYP rotational constants for the ion (see Table 4): $A_0'' = 20.95$ cm^{-1}, $B_0'' = 0.37$ cm^{-1}, $C_0'' = 0.36$ cm^{-1}. Figure 3a shows the fit of our simulation (—) and contrasts it with our observed data (···).

The NCN^- spectrum is not as simple as that of $HNCN^-$; Figure 3b clearly shows that the (0,0) peak is not a simple feature but is a composite (at least) of two bands. The NCN peak width is not consistent with a single rotational contour with $T_{rot} \cong 200$ K, and it does not change upon cooling, as one might expect for a rotational envelope. We are able to model the shape as being due to two transitions from the two spin-orbit states of NCN^- $\tilde{X}\ ^2\Pi_{u\ 1/2\ 3/2}$ state (see Figure 3b). The spin orbit splitting in the excited $\tilde{A}\ ^3\Pi_u$ state of NCN has been[11] worked out ($A_0 = -37.566\,64 \pm 0.000\,60$ cm^{-1}) and the Π state has been shown[10,11] to be inverted, $\tilde{A}$ NCN $^3\Pi_{u\ 3/2}$. The neutral that is isoelectronic with the NCN^- ion is NCO and it is established[36] that $A = -96.7 \pm 1.5$ cm^{-1}. We estimate that the spin orbit splitting in the NCN^- ion is $|A| = 77 \pm 33$ cm^{-1}. Adopting (a) the known rotational constant for NCN $\tilde{X}\ ^3\Sigma_g^-$ in Table 1 [$B_0' = 0.397\,252\,2$ cm^{-1}], (b) $T_{rot} = 200$ K, and (c) an instrumental linewidth (FWHM) of 10 meV, we can reproduce the 16 meV FWHM band for NCN^- in Figure 3a if we adopt the B3LYP rotational constant for the ion (see Table 4): $B_0'' = 0.40$ cm^{-1} and $|A| = 77 \pm 33$ cm^{-1}.

At the bottom of Table 3, we list the final corrected electron affinities for both ions: EA($\tilde{X}\ ^3\Sigma_g^-$ NCN) = 2.484 ± 0.006 eV, EA($\tilde{X}\ ^2A''$ HNCN) = 2.622 ± 0.005 eV, and EA($\tilde{X}\ ^2A''$ DNCN) = 2.622 ± 0.005 eV.

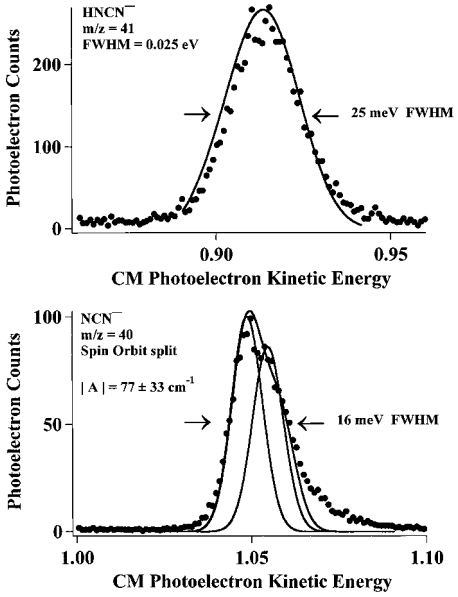

Figure 3. (a) Rotational simulation (—) of the (0,0) band of $HNCN^-$ and comparison with the observed data (···). The simulation adopts (a) rotational constants for HNCN $\tilde{X}\ ^2A''$ ($A_0' = 21.2 \pm 0.1$ cm^{-1}, $B_0' = 0.369\,849\,6 \pm 0.000\,000\,3$ cm^{-1}, $C_0' = 0.362\,974\,8 \pm 0.000\,000\,3$ cm^{-1}), (b) rotational constants for $HNCN^-$ $\tilde{X}\ ^1A'$ ion ($A_0'' = 20.95$ cm^{-1}, $B_0'' = 0.37$ cm^{-1}, $C_0'' = 0.36$ cm^{-1}), (c) $T_{rot} = 200$ K, and (d) an instrumental linewidth (FWHM) of 10 meV. (b) Rotational simulation (—) of the (0,0) band of NCN^- and comparison with the observed data (···). The simulation adopts the known rotational constant for NCN $\tilde{X}\ ^3\Sigma_g^-$ ($B_0' = 0.397\,252\,2$ cm^{-1}), (b) the rotational constant for the NCN^- ion ($B_0'' = 0.40$ cm^{-1} and $|A| = 77 \pm 33$ cm^{-1}), (c) $T_{rot} = 200$ K, and (d) an instrumental linewidth (FWHM) of 10 meV.

We are not able to detect any excited electronic states of NCN and HNCN, but we can place a lower bound on the splitting between the ground and excited states of each radical. The EA-

TABLE 5: Complete Basis Set Calculated *Ab Initio* Electronic Energies

molecule	state	method	energy/hartree	ΣD_0/kcal mol^{-1}	$\Delta_f H_0$/kcal mol^{-1}	$\Delta_f H_{298}$/kcal mol^{-1}
NCN	$^1\Delta_g$	CBS-4	−147.240 39	253.0 ± 2.5	142.1 ± 2.5	142.3 ± 2.5
		CBS-Q	−147.239 21	259.5 ± 1.3	135.5 ± 1.3	135.8 ± 1.3
		CBS-QCI/APNO	−147.424 28	258.2 ± 0.7	136.9 ± 0.7	137.1 ± 0.7
	$^3\Sigma_g^-$	CBS-4	−147.296 43	288.1 ± 2.5	106.9 ± 2.5	107.0 ± 2.5
		CBS-Q	−147.286 47	289.2 ± 1.3	105.9 ± 1.3	106.1 ± 1.3
		CBS-QCI/APNO	−147.470 19	287.0 ± 0.7	108.1 ± 0.7	108.2 ± 0.7
NCN^-	$^2\Pi_u$	CBS-4	−147.391 44			
		CBS-Q	−147.378 00			
		CBS-QCI/APNO	−147.562 67			
HNCN	$^2A''$	CBS-4	−147.930 65	370.3 ± 2.5	76.4 ± 2.5	75.8 ± 2.5
		CBS-Q	−147.915 84	370.5 ± 1.3	76.2 ± 1.3	75.6 ± 1.3
		CBS-QCI/APNO	−148.101 27	369.3 ± 0.7	77.4 ± 0.7	76.7 ± 0.7
$HNCN^-$	$^1A'$	CBS-4	−148.025 95			
		CBS-Q	−148.009 80			
		CBS-QCI/APNO	−148.196 85			
H_2NCN	$^1A'$	CBS-4	−148.578 91	461.2 ± 2.5	37.1 ± 2.5	35.6 ± 2.5
		CBS-Q	−148.563 34	463.1 ± 1.3	35.2 ± 1.3	33.6 ± 1.3
		CBS-QCI/APNO	−148.751 12	463.3 ± 0.7	35.0 ± 0.7	33.4 ± 0.7

TABLE 6

	CBS *ab initio* calculated property/kcal mol^{-1}			
	CBS-4	CBS-Q	CBS-QCI/APNO	experimental/kcal mol^{-1}
D_0(H−NHCN)	93.1 ± 2.5	92.7 ± 1.3	94.0 ± 0.7	95.4 ± 3.0 (16)
$\Delta_{acid}H_{298}$(H−NHCN)	348.4 ± 2.5	348.8 ± 1.3	349.5 ± 0.7	350 ± 3 (17)
EA(HNCN)	59.8 ± 2.5	59.0 ± 1.3	60.0 ± 0.7	60.5 ± 0.2 (18)
D_0(HNCN)	82.2 ± 2.5	81.3 ± 1.3	82.3 ± 0.7	81.6 ± 1.9 (19)
$\Delta_{acid}H_{298}$(HNCN)	339.8 ± 2.5	338.9 ± 1.3	339.4 ± 0.7	− (20)
EA(NCN)	59.6 ± 2.5	57.4 ± 1.3	58.0 ± 0.7	57.3 ± 0.1 (21)

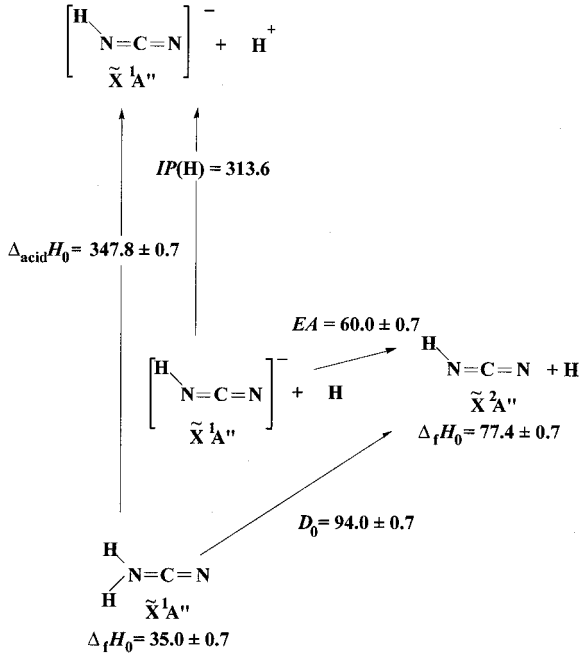

Figure 4. Calculated CBS-QCI/APNO *ab initio* thermochemical cycle for H_2NCN.

(NCN) of 2.484 eV suggests that the $\tilde{a}\ ^1\Delta_g$ state of NCN is at least 0.85 eV higher or $T_0(\tilde{a}\ ^1\Delta_g) \geq 0.85$ eV. Likewise we estimate that the $T_0(\tilde{A}\ ^2A'$ HNCN) is at least 0.70 eV above the HNCN $\tilde{X}\ ^2A''$ state. This is consistent with the LIF findings (in Table 2) that report $T_0(\tilde{A}\ ^2A'$ HNCN) = 3.594 770 ± 0.000 002 eV.

IV. Thermochemistry

The chemistry and spectroscopy of negative ions provides a useful avenue to extract a number of thermochemical parameters.[37] If one can measure the enthalpy of deprotonation for a species RH [$\Delta_{acid}H_{298}$(RH)] and separately find the electron affinity of the corresponding radical [EA(R)], then a simple cycle that uses the ionization potential of H atom can provide a value for the bond enthalpy [DH_{298}(RH)].

$$\Delta_{acid}H_{298}(RH) = DH_{298}(RH) + IP(H) - EA(R) - \int_0^{298} dT[C_p(R) - C_p(R^-) + C_p(H) - C_p(H^+)] \quad (10)$$

Since the sum of the integrated heat capacities is always[37] small (≤0.3 kcal mol^{-1}), the term in brackets will be ignored and we will use a more common expression, $\Delta_{acid}H_{298}(RH) \cong DH_{298}(RH) + IP(H) - EA(R)$. The gas phase acidity for cyanamide has been measured[38,39] in a flowing afterglow device, and the enthalpy of deprotonation was reported to be $\Delta_{acid}H_{298}$(H−NHCN) = 350 ± 2 kcal mol^{-1}. A separate set of ion experiments[40] were interpreted to yield $\Delta_{acid}H_{298}$(H−NHCN) = 349.8 ± 4 kcal mol^{-1}. Use of our electron affinity, EA(HNCN) = 60.5 ± 0.1 kcal mol^{-1}, leads to a value for the bond enthalpy of cyanamide, DH_{298}(H−NHCN) = 96.7 ± 2.3 kcal mol^{-1}. The bond enthalpy at 298 K and the bond energy at 0 K are related by the heat capacities.

$$DH_{298}(RH) = D_0(RH) + \int_0^{298} dT[C_p(R) + C_p(H) - C_p(RH)] \cong D_0(RH) + \int_0^{298} dT\, C_p(H) \quad (11)$$

Since the integrated heat capacity for H atom is just $^5/_2$RT, we find D_0(H−NHCN) = 95.2 ± 2.3 kcal mol^{-1}. The most reliable heat of formation for cyanamide[41] that we have found is $\Delta_f H_{298}(NH_2CN)$ = 32 ± 2 kcal mol^{-1}. Consequently our value for DH_{298}(H−NHCN) leads to $\Delta_f H_{298}$(HNCN) = 77 ± 3 kcal mol^{-1}.

If we can estimate the acidity of the HNCN radical, we could extract the second NH bond enthalpy of cyanamide, DH_{298}(H−NCN).

$$\Delta_{acid}H_{298}(H-NCN) \cong DH_{298}(H-NCN) + IP(H) - EA(NCN) \quad (12)$$

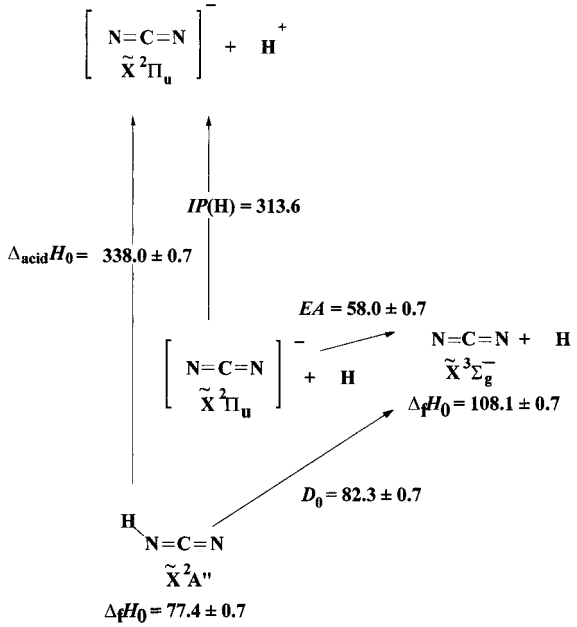

Figure 5. Calculated CBS-QCI/APNO *ab initio* thermochemical cycle for HNCN.

The acidity of the cyanoamino radical is not yet experimentally available, so we adopt a computational estimate extracted from our CBS *ab initio* electronic structure calculations (*vide infra*), $\Delta_{acid}H_{298}$(H−NCN) = 339.4 ± 0.7 kcal mol^{-1}. Use of our experimental electron affinity, EA(NCN) = 57.3 ± 0.1 kcal mol^{-1}, leads to the NH bond enthalpy of the cyanoamino radical, DH_{298}(H−NCN) = 83.2 ± 1.0 kcal mol^{-1} and D_0(H−NCN) = 81.7 ± 1.0 kcal mol^{-1}. From our value for Δ_fH_{298}(HNCN), we can use DH_{298}(H−NCN) to extract Δ_fH_{298}(NCN) = 107.7 ± 3.2 kcal mol^{-1}. JANAF tabulates[42] a value of Δ_fH_{298}(NCN) = 112.8 ± 5.0 kcal mol^{-1}. The CBS calculations give Δ_fH_{298}(NCN) = 108.2 ± 0.7 kcal mol^{-1}.

Since the thermochemistry of many small radicals (N, C, NH, NH_2, CN) is known,[42,37] one can assemble an entire family of bond enthalpies, DH_{298}(RH)/kcal mol^{-1}.

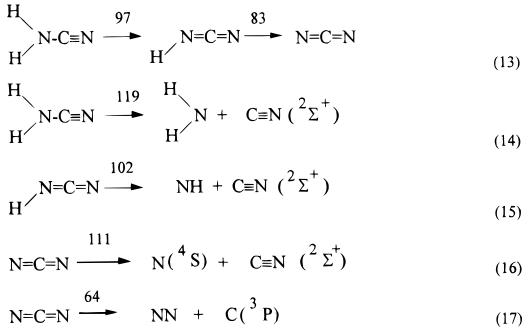

V. Complete Basis Set *Ab Initio* Electronic Structure Calculations

All of the GVB formulae in (2)−(6) are qualitatively correct. That is to say that the shapes of the radicals and ions are correct, as is the order of the electronic states. The rotational constants and harmonic vibrational frequencies are also faithfully rendered by the HF-MP2 and DFT-B3LYP calculations. The small number of atoms in the two systems allowed us to perform the full range of computationally intensive CBS calculations.[2−4] These compound models employ modest basis sets for the geometry and frequency calculations, large basis sets for a single point SCF calculation, medium basis sets for the MP2 correction with extrapolation to the CBS limit, and small basis sets for higher orders of perturbation theory. The most demanding CBS-QCI/APNO model employs atomic pair natural orbital (APNO) basis sets, while the CBS-Q model goes up to QCISD(T)/6-31+G†† calculations and the CBS-4 model tops off at MP4/6-31G. These CBS-QCI/APNO, CBS-Q, and CBS-4 models are applicable to systems with up to 4, 8, and 16 many-electron atoms with root mean square (rms) errors of ±0.7, ±1.3, and ±2.5 kcal mol^{-1}, respectively.[2−4] The results are summarized in Table 5 where the uncertainties quoted are the rms errors from the G2 test set.[43] The agreement between our experimental findings and the results of modern *ab initio* electronic structure calculations is excellent. The performance of the relatively inexpensive CBS-4 model is particularly encouraging. Table 6 compares the results.

The NCN^- CBS-QCI/APNO results are shown in Figure 4 while those for $HNCN^-$ are displayed in Figure 5. All calculations employed a modified version of the Gaussian 94 suite of *ab initio* electronic structure programs.[4]

Acknowledgment. G.B.E. is supported by a grant from the Chemical Physics Program, United States Department of Energy (DE-FG02-87ER13695); W.C.L. thanks the National Science Foundation for grant support CHE97-03486 and PHY95-12150. The collaboration between G.B.E. and G.A.P. is *via* PRF 30676-AC6. Acknowledgment is made to the Donors of the Petroleum Research Fund, administered by the American Chemical Society, for partial support of this research. G.A.P. receives support through a grant from Gaussian, Inc. To carry out the Gaussian 94 *ab initio* electronic structure calculations, we have used a cluster of RSC-6000 digital computers supported by NSF CHE-9412767. Throughout this work, we have benefited greatly from the insight of Prof. Steven Kass. We would particularly like to thank Prof. Geoffrey Duxbury for many fruitful discussions about the spin-orbit and Renner−Teller effects.

References and Notes

(1) Jennings, K. R.; Linnett, J. W. *Trans. Faraday Soc.* **1960**, *56*, 1737.
(2) Montgomery Jr., J. A.; Ochterski, J. W.; Petersson, G. A. *J. Chem. Phys.* **1994**, *101*, 5900.
(3) Ochterski, J. W.; Petersson, G. A.; Montgomery, J. A., Jr. *J. Chem. Phys.* **1996**, *104*, 2598.
(4) Frisch, M. J.; Trucks, G. W.; Schlegel, H. B.; Gill, P. M. W.; Johnson, B. G.; Robb, M. A.; Cheeseman, J. R.; Keith, T.; Petersson, G. A.; Montgomery, J. A.; Raghavachari, K.; Al-Laham, M. A.; Zakrzewski, V. G.; Ortiz, J. V.; Foresman, J. B.; Cioslowski, J.; Stefanov, B. B.; Nanayakkara, A.; Challacombe, M.; Peng, C. Y.; Ayala, P. Y.; Chen, W.; Wong, M. W.; Andres, J. L.; Replogle, E. S.; Gomperts, R.; Martin, R. L.; Fox, D. J.; Binkley, J. S.; Defrees, D. J.; Baker, J.; Stewart, J. P.; Head-Gordon, M.; Gonzalez, C.; Pople, J. A. Gaussian 94; Revision C.2 ed.; Gaussian, Inc.: Pittsburgh, PA, 1996.
(5) Goddard, W. A., III; Harding, L. B., *Ann. Rev. Phys. Chem.* **1978**, *29*, 363.
(6) Neumark, D. M.; Lykke, K. R.; Andersen, T.; Lineberger, W. C. *J. Chem. Phys.* **1985**, *83*, 4364.
(7) Al-Za'al, M.; Miller, H. C.; Farley, J. W. *Phys. Rev. A.* **1987**, *35*, 1099.
(8) Herzberg, G. H. *Molecular Spectra and Molecular Structure: Electronic Spectra and Electronic Structure of Polyatomic Molecules*; D. Van Nostrand: Princeton, New Jersey, 1967; Vol. III.
(9) Wickham-Jones, C. T.; Ervin, K. M.; Ellison, G. B.; Lineberger, W. C. *J. Chem. Phys.* **1989**, *91*, 2762.
(10) Herzberg, G.; Travis, D. N. *Can. J. Phys.* **1964**, *42*, 1658.
(11) Beaton, S. A.; Ito, Y.; Brown, J. M. *J. Mol. Spectrosc.* **1996**, *178*, 99.
(12) Wasserman, E.; Barash, L.; Yager, W. A. *J. Am. Chem. Soc.* **1965**, *87*, 2075.
(13) Kroto, H. W. *J. Chem. Phys.* **1966**, *44*, 831.
(14) Kroto, H. W.; Morgan, T. F.; Sheena, H. H. *Trans. Faraday Soc.* **1970**, *66*, 2237.
(15) Basco, N.; Yee, K. K. *Chem. Commun.* **1968**, *3*, 150.
(16) Smith, G. P.; Copeland, R. A.; Crosley, D. R. *J. Chem. Phys.* **1989**, *91*, 1987.
(17) Milligan, D. E.; Jacox, M. E.; Comeford, J. J.; Mann, D. E. *J. Chem. Phys.* **1965**, *43*, 756.

(18) Milligan, D. E.; Jacox, M. E.; Bass, A. M. *J. Chem. Phys.* **1965**, *43*, 3149.
(19) Milligan, D. E.; Jacox, M. E. *J. Chem. Phys.* **1966**, *45*, 1387.
(20) McNaughton, D.; Metha, G. F.; Tay, R. *Chem. Phys.* **1995**, *198*, 107.
(21) Thomson, C. *J. Chem. Phys.* **1973**, *58*, 841.
(22) Berthier, G.; Kurdi, L. *C. R. Acad. Sci. Paris* **1984**, *299*, 1171.
(23) Suter, H. U.; Huang, M.-B.; Engels, B. *J. Chem. Phys.* **1994**, *101*, 7686.
(24) Herzberg, G.; Warsop, P. A. *Can. J. Phys.* **1963**, *41*, 286.
(25) Wu, M.; Hall, G.; Sears, T. J. *J. Chem. Soc. Faraday Trans.* **1993**, *89*, 615.
(26) Tao, F.-M.; Klemperer, W.; McCarthy, M. C.; Gottlieb, C. A.; Thaddeus, P. *J. Chem. Phys.* **1994**, *100*, 3691.
(27) Leopold, D. G.; Murray, K. K.; Stevens Miller, A. E.; Lineberger, W. C. *J. Chem. Phys.* **1985**, *83*, 4849.
(28) Ervin, K. M.; Lineberger, W. C. Negative, "Ion Photoelectron Spectroscopy". In *Gas Phase Ion Chemistry*; Adams, N. G., Babcock, L. M., Eds.; JAI Press: Greenwich, CT, 1992.
(29) Lee, J.; Grabowski, J. J. *Chem. Rev.* **1992**, *92*, 1611.
(30) Neumark, D. M.; Lykke, K. R.; Andersen, T.; Lineberger, W. C. *Phys. Rev. A* **1985**, *32*, 1890. EA(O) = 11 784.645 ± 0.006 cm^{-1} or 1.461 110 ± 0.000 001 eV.
(31) Siegel, M. W.; Celotta, R. J.; Hall, J. L.; Levine, J.; Bennett, R. A. *Phys. Rev.* **1972**, *A6*, 607.
(32) Cooper, J.; Zare, R. N. *J. Chem. Phys.* **1968**, *48*, 942.
(33) Gunion, R. F. *Ultraviolet Photoelectron Spectroscopy of Molecular Anions*. Ph.D. thesis, University of Colorado, 1995.
(34) Becke, A. D. *J. Chem. Phys.* **1993**, *98*, 5648.
(35) Harmony, M. D.; Laurie, V. W.; Kuczkowski, R. L.; Schwendeman, R. H.; Ramsay, D. A.; Lovas, F. J.; Lafferty, W. J.; Maki, A. G. *J. Phys. Chem. Ref. Data* **1979**, *8*, 619. It is helpful to know the experimental bond lengths for some carbon/nitrogen bonds: $r_e(N{\equiv}N)$ = 1.098 Å, $r_e(C{\equiv}N)$ = 1.172 Å, $r_e(HC{\equiv}N)$ = 1.153 Å, $r_e(HN{\equiv}C)$ = 1.172 Å, $r_e(H_2CN{=}N)$ = 1.140 Å, r_e(*trans*-HN=NH) = 1.252 Å, $r_e(H_2C{=}NN)$ = 1.300 Å, $r_e(H_2C{=}NH)$ = 1.273 Å, $r_e(H_3C{-}NH_2)$ = 1.471 Å.
(36) Jacox, M. E. *Vibrational and Electronic Energy Levels of Polyatomic Transient Molecules*; American Institue of Physics: Woodbury, NY, 1994.
(37) Berkowitz, J.; Ellison, G. B.; Gutman, D. *J. Phys. Chem.* **1994**, *98*, 2744.
(38) Kroeker, R. L.; Kass, S. R. *J. Am. Chem. Soc.* **1990**, *112*, 9024.
(39) Kass, S. R. (privately communicated).
(40) Cacace, F.; de Petris, G.; Grandinetti, F.; Occhiucci, G. *J. Phys. Chem.* **1993**, *97*, 4239.
(41) Lias, S. G.; Bartmess, J. E.; Liebman, J. F.; Holmes, J. L.; Levin, R. D.; Mallard, W. G. *J. Phys. Chem. Ref. Data* **1988**, *17 (supplement 1)*, 1.
(42) Chase, M. W., Jr.; Davies, C. A.; Downey, J. R., Jr.; Frurip, D. J.; McDonald, R. A.; Syverud, A. N. *J. Phys. Chem. Ref. Data* **1985**, *14* (Supplement No. 1), 1 (JANAF Thermochemical Tables).
(43) Curtiss, L. A.; Raghavachari, K.; Trucks, G. W.; Pople, J. A. *J. Chem. Phys.* **1991**, *94*, 7221.
(44) Hensel, K. D.; Brown, J. M. *J. Mol. Spectrosc.* **1996**, *180*, 170.
(45) Martin, J. M. L.; Taylor, P. R.; Francois, J. P.; Gijbels, R. *Chem. Phys. Lett.* **1994**, *226*, 475.
(46) Yamamoto, S.; Saito, S. *J. Chem. Phys.* **1994**, *101*, 10350.
(47) Engelking, P. C. *J. Phys. Chem.* **1986**, *90*, 4544.